FIELD EXPERIENCE WITH A NEW PERFORMANCE CHARACTERIZATION PROCEDURE
FOR PHOTOVOLTAIC ARRAYS

David L. King, Jay A. Kratochvil, and William E. Boyson
Sandia National Laboratories
Albuquerque, New Mexico, 87185, USA
http://www.sandia.gov/pv/

ABSTRACT: As photovoltaic systems become larger and more numerous, improved methods are needed for testing and modeling their performance. Test methods that successfully separate the interacting, time-of-day dependent influences of solar irradiance, operating temperature, solar spectrum, and solar angle-of-incidence have now been developed. These test methods have resulted in a new array performance model that is reasonably simple, yet accurately predicts performance for all operating conditions. This paper describes the new model, outdoor tests required to implement it, results of field tests for five arrays of different technologies, and the evolution of the model into a numerical tool for designing and sizing photovoltaic arrays based on annual energy production.
Keywords: PV Array-1: Performance-2: Sizing-3

1. INTRODUCTION

The maturity of the photovoltaic industry can be gauged by its ability to design and size arrays for different applications and sites, and then to accurately and cost-effectively verify array performance in the field. These abilities will be fully manifested when they can be equitably applied to crystalline silicon, thin-film, and concentrator photovoltaic technologies, with array sizing based on either power or energy production. Current practices are not yet adequate to meet the needs of a growing PV industry.

Outdoor measurement procedures and photovoltaic performance models have evolved over many years in laboratories all over the world, and considerable effort has been spent by agencies such as ASTM, IEEE, and IEC toward standardizing test methods. Sandia has been conducting outdoor tests of module and array performance since 1976. Our work has recently led to new outdoor module testing procedures that effectively address the interacting influences mentioned in the abstract, thus providing the context for a performance model that works well for a wide range of outdoor operating conditions. Over the last three years, our module testing procedures and models have been adapted and applied with a high degree of success to a variety of large photovoltaic arrays.

Collaborative efforts are now in progress by Sandia, NREL, PVUSA, NIST, module manufacturers, system integrators, and developers of system design software to combine the best elements of different approaches. The goal of this collaboration is to arrive at consensus-based standards for testing and modeling of array performance.

2. ARRAY RATING CONDITIONS

Historically, the performance of photovoltaic (PV) cells and modules has been determined at a test condition called the "Standard Reporting Condition (SRC)," or commonly the "Standard Test Condition (STC)" [1, 2].

The SRC test condition was originally intended to mimic actual outdoor conditions, but was also modified to facilitate indoor testing procedures. As a result, the irradiance level, 1000 W/m^2, and the two "standard" solar spectral distributions [3, 4] are representative of typical clear-sky operating conditions, but the 25°C cell temperature is not. Outdoor operating conditions commonly result in cell temperatures closer to 50°C. Unfortunately, the difference between actual operating temperatures and the SRC temperature has often been a source of array design errors, marketing difficulties, and dissatisfied customers.

In lieu of a new standard, system engineers have attempted in different ways to determine array or system performance for "actual operating conditions" [5, 6].

2.1 PVUSA Test Conditions (PTC)

A government and utility sponsored activity called "Photovoltaics for Utility Scale Applications (PVUSA)" has developed and implemented a test method that relates photovoltaic system performance to the prevailing environmental conditions; solar irradiance, ambient temperature, and wind speed [5]. This method has been applied to a variety of PV technologies, can be used to determine either dc or ac performance, and uses a simple regression model. The limitations of the method include the requirement for continuous data acquisition over an extended period of time, relatively poor accuracy of the model for low irradiance levels, and it does not explicitly address the systematic influences of solar spectral and angle-of-incidence variation [7].

2.2 New Array Rating Methodology

At the risk of introducing additional confusion, the authors would like to propose an array rating methodology that combines a specific "array rating condition" (ARC) with a method for calculating performance at other "specified operating conditions" (SOC). This approach should meet the needs of the system owner who may have a variety of specific operating conditions of importance. In addition, the specific array rating condition chosen should be consistent with traditional PV testing standards and meets the needs of the metrologist tasked with field performance verification. The ARC is the same as the

DISCLAIMER

DISCLAIMER

Portions of this document may be illegible electronic image products. Images are produced from the best available original document.

traditional standard reporting condition (SRC) with the exception that the cell temperature used as a reference, T_o, is raised to a value more representative of actual operating conditions for the module being evaluated.

Ideally, the array rating methodology should not only provide a rating at the ARC and performance estimates at a variety of SOC, but also provide the information required to accurately estimate the annual energy production from the PV system. The results in this paper describe our progress toward this ideal goal.

3. NEW PV PERFORMANCE MODEL

Photovoltaic array performance parameters, for an arbitrary operating condition, can be described using Eqns. (1-5). The variables defining the operating condition are irradiance, cell temperature, absolute air mass, and solar angle-of-incidence on the array. The equations for short-circuit current (I_{sc}), maximum-power current (I_{mp}), open-circuit voltage (V_{oc}), and maximum-power voltage (V_{mp}) provide the four primary parameters from which others (fill factor, maximum power, efficiency) can be calculated. Eqns. (1, 3, and 4) result in linear relationships closely related to the fundamental electrical characteristics of cells in the module. Eqn. (5) uses a second order relationship for V_{mp} that implicitly contains the influence of factors such as series resistance (R_s) and non-ideal shunting behavior (R_{sh}, n_2) of cells at low irradiance levels. Two additional empirical relationships, $f_1(AM_a)$ and $f_2(AOI)$, are used to compensate for the influences of the solar spectrum and solar angle-of-incidence (AOI) on the short-circuit current.

A fundamental premise of this performance model is that the I_{mp}, V_{mp}, and V_{oc} of a cell, module, or array are predictable parameters when described as functions of I_{sc} and cell temperature (T_c) only. In other words, for a given I_{sc} and T_c, the shape of the current-voltage (I-V) curve will be the same for any solar spectrum and angle-of-incidence. When this premise is valid, the performance characterization of an array becomes simply a matter of first determining the short-circuit current, I_{sco}, at the array rating condition. Then the other three performance parameters are measured and related to I_{sco} using the "effective irradiance" term (E_e) in Eqn. (2). The concept of "effective irradiance" is used in ASTM methods [8] to account for the fact that photovoltaic devices do not respond to all wavelengths of light contained in the solar spectrum. As used in this paper, the term is expanded to include not only the solar spectral influence, but also the optical effects related to solar angle-of-incidence. Thus, the effective irradiance, E_e, in Eqn. (2) depends on both the solar spectrum and the solar angle-of-incidence.

One advantage of this approach is that compensating for the effects of solar spectrum and solar angle-of-incidence can be accomplished by adjusting only the I_{sc} parameter in Eqn. (1). In addition, the model is easily adapted, if necessary, to special cases. For instance, if a module requires a second spectral correction function to more closely model I_{mp} at low irradiance (high AM_a) conditions, it can be applied to E_e in Eqn. (3).

$$I_{sc}(E, T_c, AM_a, AOI) =$$
$$(E/E_o)\, f_1(AM_a)\, f_2(AOI)\, \{I_{sco} + \alpha_{Isc}(T_c - T_o)\} \quad (1)$$

$$E_e = I_{sc}(E, T_c = T_o, AM_a, AOI) / I_{sco} \quad (2)$$

$$I_{mp}(E_e, T_c) = C_0 + E_e\{C_1 + \alpha_{Imp}(T_c - T_o)\} \quad (3)$$

$$V_{oc}(E_e, T_c) = V_{oco} + C_2 \ln(E_e) + \beta_{Voc}(T_c - T_o) \quad (4)$$

$$V_{mp}(E_e, T_c) = V_{mpo} + C_3 \ln(E_e) + C_4\{\ln(E_e)\}^2 + \beta_{Vmp}(T_c - T_o) \quad (5)$$

Where:
E = plane-of-array (POA) solar irradiance using broadband (thermopile) pyranometer measurement corrected for angle-of-incidence sensitivity, W/m^2
E_e = "effective" irradiance, dimensionless, or "suns"
$\ln(E_e)$ = natural logarithm of E_e
E_o = reference "one sun" irradiance on array, 1000 W/m^2
AM_a = absolute air mass, dimensionless
AOI = solar angle-of-incidence on module, degrees
T_c = temperature of cells inside module, °C
T_o = reference temperature for cells in module, e.g. 50 °C
$f_1(AM_a)$ = empirically determined "AM_a-Function" describing solar spectral influence on I_{sc}
$f_2(AOI)$ = empirically determined "AOI-Function" describing angle-of-incidence influence on I_{sc}
$I_{sco} = I_{sc}(E = 1000$ W/m^2, $AM_a = 1.5$, $T_c = T_o$ °C, AOI = 0°)
$I_{mpo} = I_{mp}(E_e = 1, T_c = T_o$°C)
$V_{oco} = V_{oc}(E_e = 1, T_c = T_o$ °C)
$V_{mpo} = V_{mp}(E_e = 1, T_c = T_o$ °C)
$\alpha_{Isc} = I_{sc}$ temperature coefficient, A/°C
$\alpha_{Imp} = I_{mp}$ temperature coefficient, A/°C
$\beta_{Voc} = V_{oc}$ temperature coefficient, V/°C
$\beta_{Vmp} = V_{mp}$ temperature coefficient, V/°C
C_0, C_1 = empirical coefficients relating I_{mp} to irradiance
C_2 = empirical coefficient relating V_{oc} to irradiance
C_3, C_4 = empirical coefficients relating V_{mp} to irradiance

4. MODULE PERFORMANCE

The first step toward achieving a comprehensive array performance characterization is to accurately determine the performance characteristics of the modules used in the array. This section summarizes outdoor test procedures that can be used for this process.

4.1 Solar Irradiance Measurements
Historically, one of the largest contributors to the uncertainty in field measurements of array performance has been error in measurements of the solar irradiance. The irradiance measurements are used to translate array performance data to a reference irradiance level. So, errors in irradiance measurements translate directly into errors in array performance ratings. Particular attention must be paid to the angle-of-incidence sensitivity of the pyranometer being used, and if silicon-based pyranometers are used, then solar spectral influence must be addressed [9]. With appropriate correction for these systematic influences, solar irradiance measurements with a total uncertainty of less than 3% should be achievable using typical instruments.

4.2 Temperature Coefficients
Two temperature coefficients, one for current and one for voltage, are currently used in ASTM standard methods for translating measured current-voltage (I-V) curves from

one temperature to another [2]. Our experience has indicated that improved accuracy in performance modeling can be achieved by recognizing that the temperature coefficients for current and voltage at the maximum-power point can differ significantly from those obtained at short-circuit and open-circuit conditions [10]. As a result, the performance model previously presented uses four separate temperature coefficients. The common practice of using a single temperature coefficient for power, or efficiency, should also be avoided.

4.3 Solar Spectral Influence

Compensation for the influence of time-of-day dependent solar spectral variation was achieved by using an empirically determined function. The method for determining this function was documented elsewhere [11]. This empirical function, $f_1(AM_a)$, related solar spectral influence on I_{sc} to the absolute air mass (AM_a). Fig. 1 illustrates the empirical relationships measured for several commercial PV modules, including crystalline and multi-crystalline silicon (c-Si and mc-Si), amorphous silicon (a-Si), silicon film, and cadmium telluride (CdTe). Experience has indicated that, for clear sky conditions, the $f_1(AM_a)$ function is widely applicable to different sites. The coefficients, A_i, in Table I provide polynomial fits to the measured data shown in Fig. 1.

For further clarification, "air mass" is the term used to describe the path length that sunlight traverses through the atmosphere before reaching the ground. When air mass is adjusted for the altitude of the site, it is called the "absolute" air mass (AM_a). AM_a is readily calculated knowing the zenith angle of the sun and the site altitude [12], as indicated in Eqns. (6-8). At sea level, $AM_a=1$ when the sun is directly overhead, $AM_a=1.5$ when the sun's zenith angle is 48 degrees, and AM_a of about 10 is achieved at sunrise and sunset. As AM_a increases, the spectral distribution of sunlight shifts to longer wavelengths, becoming more "red."

$$AM = \left[\cos(Z_s) + 0.5057 \cdot (96.080 - Z_s)^{-1.634}\right]^{-1} \quad (6)$$

$$AM_a = \frac{P}{P_o} \cdot AM \quad (7)$$

$$\frac{P}{P_o} \approx e^{(-.0001184 \cdot h)} \quad (8)$$

Where:

AM = atmospheric optical air mass
AM_a = absolute (pressure corrected) air mass
Z_s = zenith angle of the sun, degrees
P = local atmospheric pressure, mmHg
P_o = standard pressure at sea level, 760 mmHg
h = site altitude, m

The concept of the empirical $f_1(AM_a)$ function can be understood by examining the standard ASTM method [13] for calculating the "spectral mismatch correction" parameter, M, shown mathematically in Eqn. (9).]. When a thermopile (broadband) pyranometer is used as the reference irradiance sensor, the simpler Eqn. (10) results. Our outdoor test procedure for determining $f_1(AM_a)$ provided the method used for directly measuring the spectral correction parameter as it continuously varied over the course of a day [11]. Thus, $f_1(AM_a)$ was determined by

directly measuring broadband irradiance and module short-circuit current over the a day, without the need for numerical integration or spectral irradiance measurements. The $f_1(AM_a)$ function was normalized to a value of one at the time of day when $AM_a=1.5$ occurred.
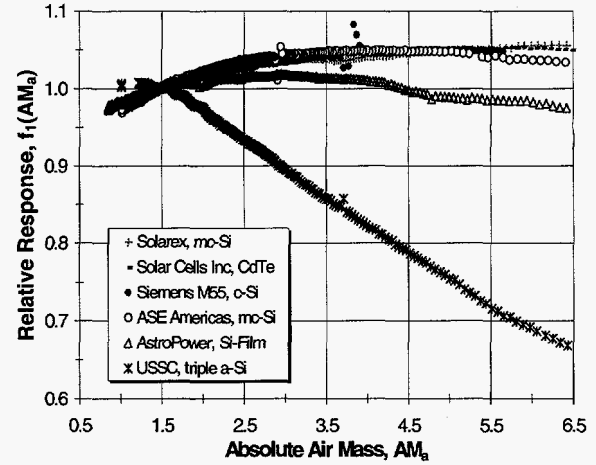

Fig. 1: Measured effect of solar spectral variation (AM_a) on the relative response (short-circuit current) of different commercial modules, for clear sky conditions.

Table I: Polynomial coefficients required for modeling spectral and AOI influence on module performance.

Coef	ASE300 (EFG-Si)	SM55 & MSX120	AP8225 (Si-Film)	SCI (CdTe)	US64 (a-Si)
A_0	.875	.928	.915	.891	.976
A_1	1.221E-1	6.796E-2	9.282E-2	9.907E-2	8.250E-2
A_2	-3.019E-2	-1.507E-2	-2.819E-2	-2.239E-2	-5.707E-2
A_3	3.104E-3	1.587E-3	3.230E-3	2.238E-3	8.242E-3
A_4	-1.187E-4	-6.377E-5	-1.354E-4	-8.868E-5	-3.919E-4
B_0	1	1	1	1	1
B_1	-2.438E-3	-2.438E-3	-2.438E-3	-2.438E-3	-5.020E-3
B_2	3.103E-4	3.103E-4	3.103E-4	3.103E-4	5.842E-4
B_3	-1.246E-5	-1.246E-5	-1.246E-5	-1.246E-5	-2.300E-5
B_4	2.112E-7	2.112E-7	2.112E-7	2.112E-7	3.826E-7
B_5	-1.359E-9	-1.359E-9	-1.359E-9	-1.359E-9	-2.310E-9

$$M = \frac{\int_a^b E(\lambda)R_t(\lambda) \cdot d\lambda \quad \int_c^d E_o(\lambda)R_r(\lambda) \cdot d\lambda \cdot}{\int_c^d E(\lambda)R_r(\lambda) \cdot d\lambda \quad \int_a^b E_o(\lambda)R_t(\lambda) \cdot d\lambda} \quad (9)$$

$$M \approx \frac{Isc_t}{E^*} \cdot \frac{E_o^*}{Isc_{to}} = f_1(AM_a) \quad (10)$$

Where:

M = spectral correction parameter
λ = wavelength (nm)
$E(\lambda)$ = solar spectral irradiance present during test,
$E_o(\lambda)$ = reference solar spectral irradiance at prevailing $AM_a=1.5$ condition,
$R_t(\lambda)$ = spectral response of test module at reference temperature,
$R_r(\lambda)$ = spectral response of reference thermopile pyranometer,
a,b = integration limits defined by photovoltaic module,
c,d = integration limits defined by reference pyranometer,

E_o^* = total irradiance indicated by thermopile (broadband) pyranometer for normal incidence, AM_a=1.5 condition,
E^* = total irradiance indicated by thermopile pyranometer for prevailing test spectrum, normal incidence,
Isc_{to} = short-circuit current from test module at reference temperature, normal incidence, AM_a=1.5 condition,
Isc_t = measured short-circuit current at reference temperature, normal incidence, prevailing test spectrum.

4.4 Angle-of-Incidence Influence

A module's response to the direct (beam) irradiance component is influenced by the cosine of the solar angle-of-incidence, AOI, and by the optical characteristics of its front surface. The response of the module to uniformly diffuse irradiance can be assumed to have no dependence on angle-of-incidence. Algorithms for calculating the solar angle-of-incidence for both fixed and solar-tracking modules are documented elsewhere [14]. The optical influence of the module's front surface, which is typically glass, sometimes a polymer sheet, can be described by another empirically determined function, $f_2(AOI)$. The outdoor test procedure for determining the $f_2(AOI)$ function was also documented elsewhere [11]. Basically, the test procedure involves measuring the I_{sc} while moving the module through a range of AOI. Simultaneous measurements of diffuse solar irradiance (E_{diff}) in the plane of the module and direct normal irradiance (E_{dni}) provide $f_2(AOI)$, as given by Eqn. (11).

$$f_2(AOI) = \frac{\dfrac{E_o}{I_{sco}} \cdot I_{sc}(AM_a = 1.5, T = T_o) - E_{diff}}{E_{dni} \cdot \cos(AOI)} \quad (11)$$

Fig. 2 illustrates the relative response of several commercial flat-plate PV modules versus the solar angle-of-incidence. With the exception of the amorphous silicon module from United Solar Systems Corporation (USSC), all the modules had a glass front surface. The front surface of the USSC module was a stippled sheet of Tefzel™ polymer, and its AOI characteristics differed somewhat from the glass modules. It appears that a single $f_2(AOI)$ function may be applicable for most modules with glass front surfaces. The coefficients, B_i, for the polynomial fits shown in Fig. 2 are given in Table I.

4.5 Module Operating Temperature

Often during PV system design and array sizing, it is necessary to estimate module operating temperature from tabulated environmental parameters; ambient temperature, wind speed, and POA irradiance. The thermal environment that dictates module operating temperature is complex, also being influenced by wind direction and module design, orientation, and mounting structure. However, a simple model has been found to provide reasonably accurate estimates (±5°C) of module back surface temperature for typical flat-plate modules, near thermal equilibrium, mounted in an open rack structure. Eqn. (12) gives the simple relationship used. Roof-integrated modules with minimal convective cooling from the rear surface may operate at temperatures 10 to 20 °C above those in open racks.
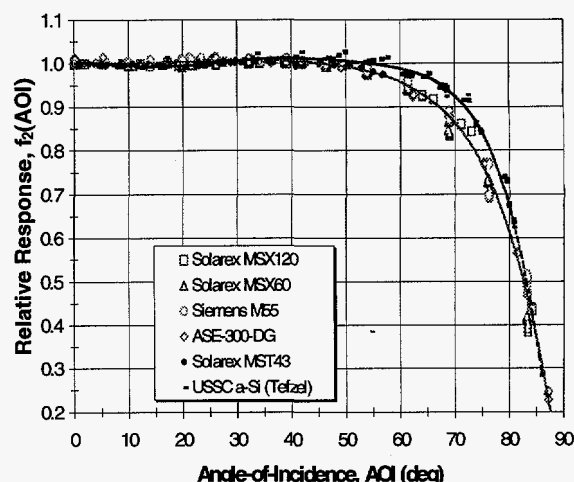

Fig. 2: Measured effect of angle-of-incidence (AOI) variation on the response (short-circuit current) of different commercial photovoltaic modules.

Module performance should actually be related to cell temperature inside the module, which is typically warmer than the back surface. The temperature difference between the cell and the back surface (ΔT) depends on the solar irradiance level and the type and thickness of the materials used for the substrate of the module. Eqn. (13) gives a simple relationship between module back-surface temperature and cell temperature. Table II gives the parameters found to give good agreement with measured temperatures for two different module types.

$$T_m = \frac{E}{E_o} \cdot \{T_1 \cdot e^{b \cdot WS} + T_2\} + T_a \quad (12)$$

Where:
T_m = back-surface module temperature, °C
T_a = ambient temperature, °C
E = solar irradiance on module, W/m^2
E_o = reference irradiance, 1000 W/m^2
WS = wind speed measured at standard 10-m height, m/s
T_1 = empirical coefficient determining upper temperature limit at low wind speeds
T_2 = empirical coefficient determining lower temperature limit at high wind speeds
b = empirical coefficient determining the rate that module temperature drops as wind speed increases

$$T_c = T_m + \frac{E}{E_o} \cdot \Delta T \quad (13)$$

Table II: Empirical coefficients for module and cell temperature estimation, for two typical module designs.

Type	T_1 (°C)	T_2 (°C)	b	ΔT (°C)
Glass/cell/glass	25.0	8.2	-.112	2
Glass/cell/Tedlar	19.6	11.6	-.223	3

5. ARRAY TEST PROCEDURE

Once performance characteristics of individual modules have been determined, array performance characterization becomes relatively straight forward. The spectral and angle-of-incidence characteristics can be applied directly for an array of modules. Module temperature coefficients are simply scaled in a manner consistent with the series/parallel configuration of modules in the array. Field tests are conducted by measuring current-voltage (I-V) curves for the array at intervals during one clear day from sunrise until sunset. Simultaneous measurements of module temperature and plane-of-array solar irradiance using an AOI-corrected thermopile pyranometer are also recorded. Analysis of the field measurements results in the coefficients (C_0, C_1, C_2, C_3, C_4) required to implement the performance model in Eqns. (1-5). When the model is applied to array data, the coefficients implicitly contain the influences of module mismatch, wiring losses, bypass diodes, and blocking diodes.

5.1 Test Results for Arrays

To illustrate the accuracy and versatility of our new performance model, the results of field measurements and analysis for five arrays of different technologies will be presented. These systems included a 25-kW ASE Americas array with EFG-silicon cells, a 1.3-kW United Solar Systems array with triple-junction a-Si cells, a 17-kW AstroPower array with Si-Film™ cells, a 11-kW Solar Cells Inc. array with CdTe cells, and a 75-kW Solarex array with mc-Si cells. Figs. 3-7 graphically illustrate the results from our field measurements, after application of $f_1(AM_a)$, $f_2(AOI)$, and temperature coefficients determined at the individual module level. In order to illustrate all the arrays in the same figures, the measured data for each parameter was "normalized" by dividing by its value at the array rating condition (ARC). In general, the new method has worked quite well, giving good agreement between measured and modeled performance over a wide range of operating conditions. For the five arrays presented, agreement between measured and modeled power was typically within less than 3%, as illustrated in Fig. 7.
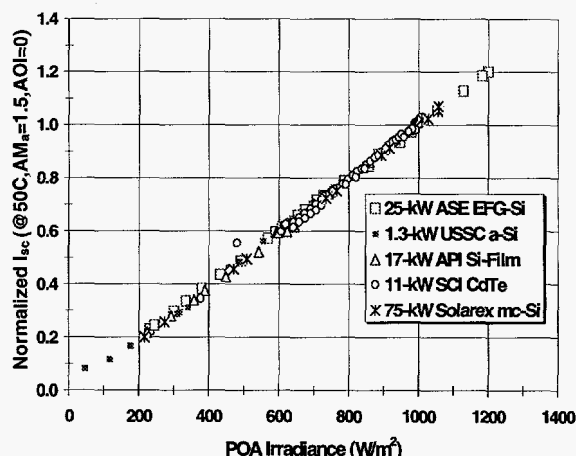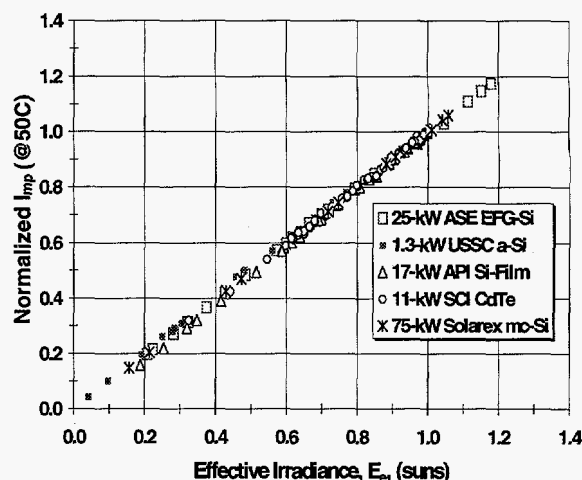

Fig. 4: Normalized I_{mp} versus effective irradiance for five arrays of different technologies, new performance model.
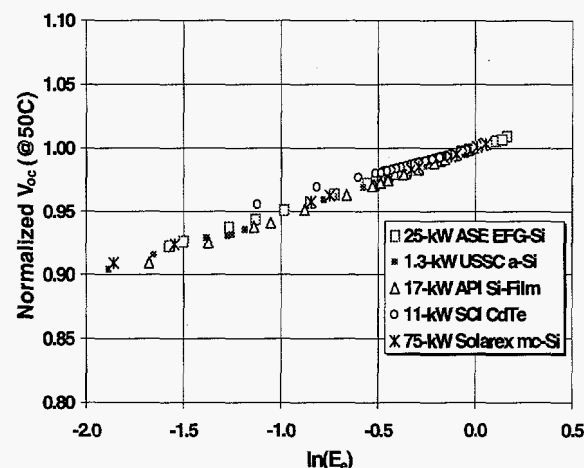

Fig. 5: Normalized V_{oc} versus logarithm of effective irradiance for five arrays, using new performance model.
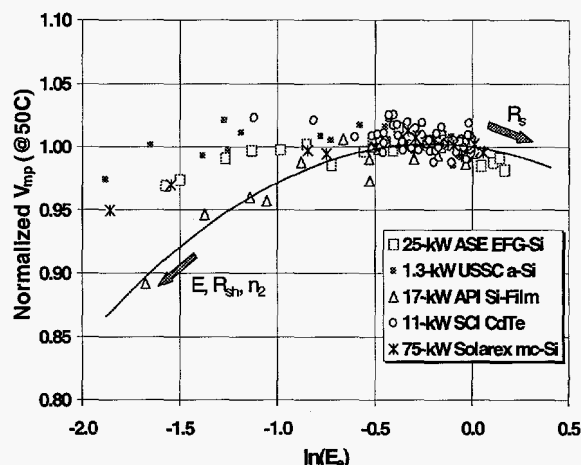

Fig. 6: Normalized V_{mp} versus logarithm of effective irradiance for five arrays, using new performance model.

Fig. 3: Normalized I_{sc} versus solar irradiance for five PV arrays of different technologies, new performance model.
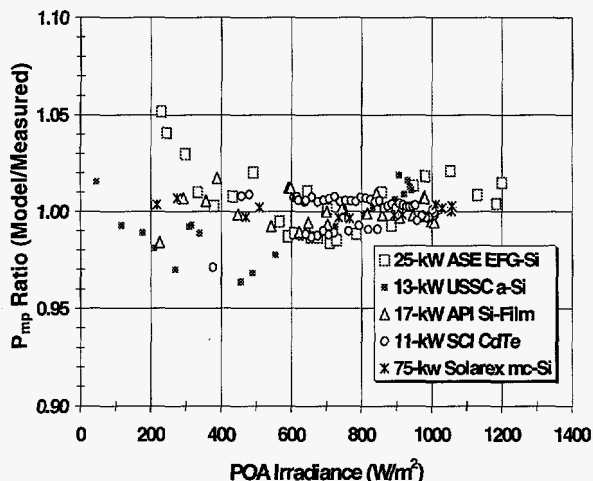
Fig. 7: Modeled P_{mp} divided by measured P_{mp} versus solar irradiance for five arrays, using new performance model.

5.2 Array Sizing for Energy Production

As a final illustration of the application of our array performance modeling methodology, Fig. 8 illustrates the predicted daily energy production (dc and ac) by month for a horizontal, roof-mounted, 100-kW array of ASE Americas modules, located in Hawaii. The array was connected to the local utility through a Trace Technologies inverter. Prior to operation, "Typical Meteorological Year (TMY2)" data were used to define the hourly average solar resource and ambient conditions, and our performance prediction accounted for the influences of irradiance, solar spectrum, AOI, calculated operating temperature, inverter efficiency, and other balance-of-system losses. After the system is operational, measured power production will be compared to predicted power providing a continuous assessment of array performance.
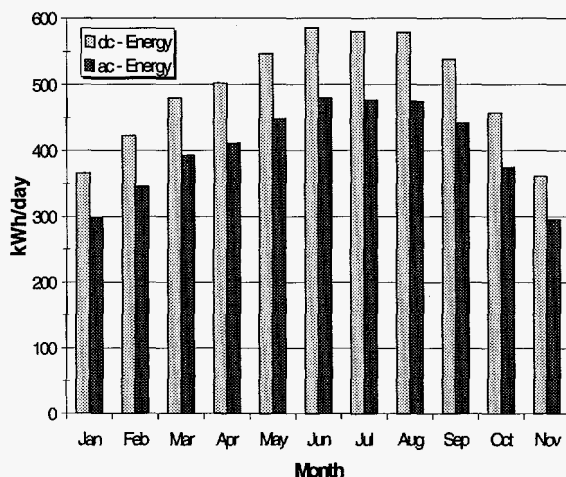

Fig. 8: Calculated daily energy production (dc and ac) for a 100-kw, roof mounted, ASE Americas array in Hawaii.

8. CONCLUSIONS

Our work has provided a significant improvement in the field testing methods and modeling procedures currently used for characterizing photovoltaic module and array performance. The array testing and modeling procedures have now been validated through field tests of 17 different arrays of nine different technologies. The new methods will improve industry's abilities to optimize system designs, to rate or specify array performance, and to monitor system performance. With industry involvement, the new modeling techniques are evolving into numerical tools for sizing systems based on either power at a specific operating condition or annual energy production.

9. ACKNOWLEDGEMENTS

10. REFERENCES

[1] ASTM E 1125, "Calibration of Silicon Non-Concentrator Terrestrial Photovoltaic Reference Cells Using a Tabular Spectrum."
[2] ASTM E 1036, "Testing Electrical Performance of Nonconcentrator Photovoltaic Modules and Arrays Using Reference Cells."
[3] ASTM E892, "Terrestrial Solar Spectral Irradiance at Air Mass 1.5 for a 37° Tilted Surface."
[4] ASTM E891, "Terrestrial Direct Normal Solar Spectral Irradiance for Air Mass 1.5."
[5] R. N. Dows, et.al., "PVUSA Procurement, Acceptance, and Rating Practices for Photovoltaic Power Plants," PG & E Co. Report #95-30910000.1, Sept. 1995.
[6] K. Bucher, et. al., "RRC Module Energy Rating: A Module Strategy," 26th IEEE PVSC, 1997, pp.1187-1191.
[7] C. M. Whitaker, et. al., "Application and Validation of a New PV Performance Characaterization Method," 26th IEEE PVSC, 1997, pp. 1253-1256.
[8] ASTM E 1039-85, "Calibration on Non-Concentrator Terrestrial PV Reference Cells Under Global Irradiation."
[9] D. King, W. Boyson, and B. Hansen, "Improved Accuracy for Low-Cost Irradiance Sensors," this conf.
[10] D. L. King, J. A. Kratochvil, and W. E. Boyson, "Temperature Coefficients for PV Modules and Arrays: Measurement Methods, Difficulties, and Results," 26th IEEE PVSC, 1997, pp.1183-1186.
[11] D. L. King, J. A. Kratochvil, and W. E. Boyson, "Measuring Solar Spectral and Angle-of-Incidence Effects on PV Modules and Solar Irradiance Sensors," 26th IEEE PVSC, 1997, pp.1113-1116.
[12] F. Kasten and A. Young, Applied Optics, 28, pp.4735-4738 (1989).
[13] ASTM E973, "Determination of the Spectral Mismatch Parameter Between a Photovoltaic Device and a Photovoltaic Reference Cell."
[14] J. A. Duffie and W. A. Beckman, Solar Engineering of Thermal Processes, 2nd Edition, Wiley & Sons, 1991.